A multiwavelength search for black widow and redback counterparts of candidate γ-ray millisecond pulsars

C. Braglia,[1] R. P. Mignani [ID],[2,3]★ A. Belfiore,[2]★ M. Marelli,[2] G. L. Israel,[4] G. Novara,[2,5] A. De Luca,[2,6]★ A. Tiengo [ID][2,5,6] and P. M. Saz Parkinson[7,8]

[1]*Department of Physics 'A. Pontremoli', University of Milan, via G. Celoria 16, I-20133 Milan, Italy*
[2]*INAF – Istituto di Astrofisica Spaziale e Fisica Cosmica Milano, via A. Corti 12, I-20133 Milan, Italy*
[3]*Janusz Gil Institute of Astronomy, University of Zielona Góra, ul Szafrana 2, PL-65-265 Zielona Góra, Poland*
[4]*INAF – Osservatorio Astronomico di Roma, via Frascati 33, I-00040 Monteporzio Catone, Italy*
[5]*Scuola Universitaria Superiore IUSS Pavia, Piazza della Vittoria 15, I-27100 Pavia, Italy*
[6]*INFN, Sezione di Pavia, via A. Bassi 6, I-27100 Pavia, Italy*
[7]*Santa Cruz Institute for Particle Physics, University of California, Santa Cruz, CA 95064, USA*
[8]*Department of Physics, Laboratory for Space Research, University of Hong Kong, Pokfulam Road, Hong Kong*

ABSTRACT

The wealth of detections of millisecond pulsars (MSPs) in γ-rays by *Fermi* has spurred searches for these objects among the several unidentified γ-ray sources. Interesting targets are a sub-class of binary MSPs, dubbed 'black widows' (BWs) and 'redbacks' (RBs), which are in orbit with low-mass non-degenerate companions fully or partially ablated by irradiation from the MSP wind. These systems can be easily missed in radio pulsar surveys owing to the eclipse of the radio signal by the intra-binary plasma from the ablated companion star photosphere, making them better targets for multiwavelength observations. We used optical and X-ray data from public data bases to carry out a systematic investigation of all the unidentified γ-ray sources from the Fermi Large Area Telescope Third Source Catalog, which have been pre-selected as likely MSP candidates according to a machine-learning technique analysis. We tested our procedure by recovering known binary BW/RB identifications and searched for new ones, finding two possible candidates. At the same time, we investigated previously proposed BW/RB identifications and we ruled out one of them based upon the updated γ-ray source coordinates.

Key words: stars: neutron – pulsars: general – gamma-rays: general – X-rays: binaries.

1 INTRODUCTION

Millisecond pulsars (MSPs) are a sub-group of radio pulsars characterized by much shorter spin periods ($P_s \lesssim 10$ ms) than the rest of the population. They are also very stable clocks, with spin period derivatives $\dot{P}_s \sim 10^{-21}$ to 10^{-18} s s^{-1}, which, according to the magnetic dipole model, imply characteristic ages $P_s/2\dot{P}_s \sim 1$–10 Gyr, low dipolar magnetic fields of $B \sim 10^8$–10^9 G, and rotational energy loss rates as low as $\dot{E} \sim 10^{32}$–10^{36} erg s^{-1}. According to the canonical recycling scenario (Alpar et al. 1982; Radhakrishnan & Srinivasan 1982), the short spin periods of MSPs are explained by a phase of matter accretion from a non-degenerate companion star, with the consequent spin-up of the neutron star. This scenario is rooted in the fact that the majority of MSPs (214/333[1]) are indeed observed in binary systems, usually with a white dwarf (WD) companion peeled off of its external layers.

The existence of *isolated* MSPs in the Galactic field (e.g. PSR B1937+21; Backer et al. 1982) then represented for a long time a conundrum. This was solved by the discovery of the MS PSR B1957+20 (Fruchter, Stinebring & Taylor 1988) in orbit around a very low-mass ($\sim 0.002\,M_\odot$) companion, with the radio signal regularly disappearing during part of the orbit. This behaviour was interpreted as an eclipse of the radio signal absorbed or scattered by intra-binary gas produced from ablation of the companion star irradiated by the pulsar wind, hence leading to the nickname 'black widow' (BW) for this pulsar. Isolated MSPs were then naturally explained as descendants of families of BW pulsars, where the companion has been fully ablated, eventually. In addition to BWs, other similar systems were discovered, starting with PSR J1023+0038 (Archibald et al. 2009), where the companion star has masses $M_C \sim 0.1$–$0.4\,M_\odot$ and is only partially ablated by irradiation from the pulsar wind. Following the spider analogy, these systems were nicknamed 'redbacks' (RBs; Roberts 2011), after the species of Australian spiders where females feed only part of their lighter male companions after mating. Both systems are characterised by very short orbital periods ($P_B < 1$ d).

These 'spiders' are crucial to understand the MSP recycling scenario and the formation of isolated MSPs, study the acceleration, composition and shock dynamics of the MSP winds, and infer accurate MSP mass measurements through pulse timing, key to determine the neutron star equation of state (see e.g. Linares 2019, for a recent review). They are elusive targets in radio pulsar surveys owing to the radio signal eclipse, with the eclipse extent unknown

[1]https://www.atnf.csiro.au/research/pulsar/psrcat/-v1.63

and variable in time. Furthermore, some RBs alternate between accretion-powered states, with high X-ray emission and no radio pulsations, and rotation-powered states, with low X-ray emission and radio pulsations (Linares 2014). The study of these 'transitional' MSPs, with only three such systems known in the Galactic field (e.g. Jaodand, Hessels & Archibald 2016, for a recent review), is key to track the long-sought evolutionary link between accreting neutron stars in low-mass X-ray binaries and MSPs in binary systems.

Since MSPs (regardless of the type) are almost half of the γ-ray pulsar population (115 out of 250, of which 91 in binary systems[2]), many of the 'spiders' known to date in the Galactic field, 43 confirmed as radio/γ-ray pulsars and 11 candidates (Linares 2019), have been searched for in unidentified γ-ray sources discovered by the *Fermi* Large Area Telescope (LAT; Atwood et al. 2009). Candidate 'spiders' are usually pinpointed through multiwavelength follow-up observations that trigger dedicated radio pulsar searches, with γ-ray pulsations searched for using the radio pulsar ephemerides, like in the case of PSR J2339−0533 (Ray et al. 2020). Much more rarely, the detection of γ-ray pulsations (Pletsch et al. 2012; Clark et al. 2017) directly triggers radio follow-ups (Ray et al. 2013). As of now, 37 'spiders' have been detected and seen to pulsate in γ-rays (Hui & Li 2019). In many cases, optical observations have been key to finding BW/RB candidates via the discovery of $\lesssim 1$ d periodic flux modulations from the tidally distorted and irradiated MSP companion, which traces the binary system orbital period (see Salvetti et al. 2015, and references therein) and facilitates radio/γ-ray pulsation searches. The quest for 'spiders' among unidentified *Fermi* sources is still restlessly pursued, with promising candidates for multiwavelength observations selected from the similarity between the γ-ray source temporal and spectral characteristics to those of known γ-ray MSPs.

In this work,[3] we assumed as a reference the candidate MSP selection done by Saz Parkinson et al. (2016) from a machine-learning analysis of unidentified γ-ray sources in the Fermi Large Area Telescope (LAT) Third Source Catalog (3FGL; Acero et al. 2015). For consistency, at this stage we did not include MSP candidates selected by independent statistical analysis of unidentified 3FGL sources, e.g. Dai et al. (2016, 2017).

Our strategy is described in Section 2, whereas the multiwavelength analysis is described in Section 3 with the results presented and discussed in Section 4. Summary and conclusions follow in Section 5.

2 STRATEGY

2.1 Candidate selection

The pulsar-like candidate list of Saz Parkinson et al. (2016) includes 120 unidentified 3FGL γ-ray sources classified in two groups: young pulsars (YNG) and MSPs. To be conservative, we considered candidates with either a non-ambiguous ('MSP/MSP'; 41) or a tentative ('MSP/YNG' or 'YNG/MSP'; 7) MSP classification. Of course, we cannot rule out that apparent mis-classifications between the two groups lead to the loss of genuine MSP candidates and to the acquisition of false ones. However, by training their algorithms on a sample of identified/associated γ-ray sources, Saz Parkinson

et al. (2016) claim an overall classification accuracy of $\gtrsim 96$ per cent, so that we expect the number of apparent mis-classifications to be limited to very few cases only. We note that since the machine-learning techniques used by Saz Parkinson et al. (2016) cannot distinguish between isolated and binary MSPs on the basis of their γ-ray temporal and spectral characteristics alone, our starting sample may very well include both isolated and binary MSP candidates. Moreover, no periodic γ-ray modulations associated with the orbital period of a compact binary system, like e.g. in 3FGL J2039.6−5618 (Ng et al. 2018), or γ-ray state transitions, like in some RBs (Torres et al. 2017), have been recognized yet for the vast majority of the above 48 MSP candidates. Therefore, we are left with no option other than applying our identification strategy, tailored on BWs and RBs, to all the 48 MSP candidates.

To test and validate our strategy, we did not filter out from our starting sample those γ-ray sources already proposed as strong BW/RB candidates prior to the publication of the work of Saz Parkinson et al. (2016), such as 3FGL 2039.6−5618 (Salvetti et al. 2015), or proposed afterwards, such as 3FGL 0954.8−3948 (Li et al. 2018), and those unambiguously identified as pulsars by the discovery of radio and/or γ-ray pulsations, such as 3FGL 1946.4−5403 (Camilo et al. 2015; Ray et al. 2016). For the same reason, we did not filter out sources that have been eventually identified as young pulsars and not as MSPs, such as 4FGL J0359.4+5414 (Clark et al. 2017), which had a tentative 'MSP/YNG' classification in Saz Parkinson et al. (2016), and we used them as false positives. In order to avoid missing potentially interesting candidates, we did not apply a cut in the MSP candidate classification ranking and we did not filter them according to their 95 per cent confidence error radius (r95). Although MSPs are expected to be found mostly at high Galactic latitudes, where they migrate owing to their proper motion in their Gyr-long lifetimes, their orbital motion in the Galactic potential can bring them back to the Galactic plane. Therefore, we did not apply a sample selection based on the source coordinates.

2.2 Multiwavelength data base

The multiwavelength identification strategy is the same as described in Salvetti et al. (2017) and applied to other BW/RB searches. Briefly, since BWs/RBs are also observed in the optical/X-rays (see e.g. Hui & Li 2019, for a compilation), this strategy consists of (i) mapping the γ-ray source error box in X-rays to spot candidate counterparts, (ii) looking for optical counterparts to the selected X-ray sources, and (iii) searching for optical modulations with periods $\lesssim 1$ d.

Since our starting sample includes 48 γ-ray sources, with a random distribution in right ascension and declination, running the multiwavelength identification effort through dedicated follow-up X-ray/optical observations for them all would be unrealistic in terms of required observing time and data analysis time investment. Therefore, we used data collected in public archives and the derived source catalogues and data products, as done in Mignani et al. (2014). In particular, in the X-rays we used the third *XMM–Newton* serendipitous source catalogue (Rosen et al. 2016) Data Release 8 (3XMM/DR8), the *Chandra* Source Catalogue (Evans et al. 2010) Release 2.0 (CSC 2.0), and the *Swift* X-ray Telescope (XRT) Point Source Catalogue (1SXPS; Evans et al. 2013). Owing to the limited number of sources (497) and to the extragalactic nature of about half of them, we did not use the *NuSTAR* Serendipitous Survey 40-month catalogue (Lansbury et al. 2017). Since we aim at looking for orbital modulations from the optical counterparts to the X-ray sources, we used multi-epoch imaging data and associated catalogues from

---

[2]https://confluence.slac.stanford.edu/display/GLAMCOG/Public+List+of+LAT-Detected+Gamma-Ray+Pulsars

[3]A more extended description can be found in C. Braglia (2020), MSc thesis Dissertation, University of Milan, Italy.

wide-area optical sky surveys. These are the Catalina Sky Survey (CSS), assembling under the same name the original CSS (Larson et al. 2003) plus its siblings the Mount Lemmon Survey (MLS) and the Siding Spring Survey (SSS), the Palomar Transient Factory (PTF; Rau et al. 2009), the intermediate Palomar Transient Factory (Kulkarni 2013), the Zwicky Transient Factory (ZTF; Bellm et al. 2018) surveys, and the Pan-Starrs survey (Chambers & Pan-STARRS Team 2016). In all cases, we used the most recent survey and data products releases. We decided not to use the recently released Hubble Catalog of Variables (Bonanos et al. 2019) because of the small sky coverage and non-uniform cadence of the multi-epoch *HST* images.

Both in the X-rays and in the optical, the choice of different catalogues/surveys is dictated by their complementarity. For instance, observations with *Swift* provide exposures for several unidentified γ-ray source fields, although they are relatively shallow, whereas observations with *XMM–Newton* provide a much sparser γ-ray source field mapping but are much deeper. Owing to the smaller field of view of its detectors, observations with *Chandra* have been rarely used to map γ-ray source fields but, when used, provide a much more accurate source positioning than both *Swift* and *XMM–Newton*, crucial for the X-ray source optical counterpart identification. In the optical, the use of different surveys yields complementary sky mappings, extended multiband flux information, more sensitive flux limits, and finer time resolution related to the different observing cadence. In addition, for sources with an already known orbital period, the use of different surveys could help detecting period variations over time, which are expected for BWs and RBs owing to the mass-loss from the companion star caused by the MSP irradiation, by comparing light curves obtained at different epochs (e.g. Cho, Halpern & Bogdanov 2018). Furthermore, different surveys also allow us to study variations in the light-curve profile as observed in different optical bands, such as in PanSTARRS, which are expected as the result of the companion star irradiation.

Of course, owing to the non-homogeneous sky mapping possible with the available survey data (especially in the X-rays, given the serendipitous nature of the surveys) some of the 48 γ-ray source fields might suffer of uneven or no multiwavelength coverage. Moreover, the catalogue releases are based on observations processed up to a certain date. This means that multiwavelength data products for a given field might not be available yet. Owing to the project's time constraints, we did not process optical/X-ray data not yet included in the most recent releases of the reference catalogues and we did not scan the entirety of public optical data archives for unprocessed data. We considered such options only on a case by case basis, depending on the preliminary results of our analysis.

Our work sets the state of the art of the multiwavelength investigation of all candidate MSPs selected from the 3FGL by Saz Parkinson et al. (2016), here carried out systematically for the first time. Some of these candidates have been already investigated by Salvetti et al. (2017) and here we have complemented their analysis using an extended multiwavelength data base.

3 MULTIWAVELENGTH ANALYSIS

3.1 Coordinate re-assessment

Before searching for X-ray and optical counterparts, we first obtained the γ-ray source positions using the recently released Fermi Large Area Telescope Fourth Source Catalog (4FGL; Abdollahi et al. 2020) based on the first 8 yr of data acquisition of the *Fermi* mission, which supersedes the Fermi LAT 8-Year Source Catalog published in 2018. We used the latest 4FGL version, released on 2019 May 15. The

4FGL data re-processing with the PASS 8 software (Bruel et al. 2018) allowed to obtain a more precise γ-ray coordinate determination and a smaller γ-ray error ellipse, which could lead to the discovery of new X-ray/optical counterparts to the γ-ray source, previously incompatible with the actual γ-ray source position. A clear example can be found in the work of Li et al. (2018), where the X-ray and optical counterparts to 3FGL J0954.8−3948 were only found after the relocalization of the γ-ray source, offset by ∼7 arcmin with respect to its original 3FGL coordinates.

Since from now on we use the 4FGL coordinates as a reference for our work, we checked how many of the MSP candidates of Saz Parkinson et al. (2016), selected from the 3FGL, are still flagged unassociated in the 4FGL. We found that nine of them have a pulsar association in the 4FGL. Two of them, 4FGL J1625.1−0020 (Salvetti et al. 2017) and 4FGL J1653.6−0158 (Romani, Filippenko & Cenko 2014), however, should still be regarded as candidates since the discovery of pulsations has not been reported yet in a dedicated paper. Of the remaining seven that are confirmed pulsars, 4FGL J0318.2+0254 (PSR J0318+0253; Wang et al. 2018), 4FGL J0359.4+5414 (PSR J0359+5414; Clark et al. 2017), 4FGL J1035.4−6720 (PSR J1035−6720; Clark et al. 2018), 4FGL J1528.4−5838 (PSR J1528−5838; Clark et al. 2017), 4FGL J1641.2−5317 (PSR J1641−5317; Clark et al. 2017), 4FGL J1744.0−7618 (PSR J1744−76194; Clark et al. 2018), and 4FGL J1946.5−5402 (PSR J1946−5403), only the last one is a binary MSP (Camilo et al. 2015). However, like we stated in Section 2, we kept these sources in our sample as a blind test of our procedure.

3.2 Cross-correlation with X-ray catalogues

First of all, we searched for candidate X-ray counterparts to the 48 γ-ray sources performing a cross-match with *XMM–Newton*, *Chandra*, and *Swift* sources that lie inside the 95 per cent confidence 4FGL error ellipse. We performed the cross-match considering only sources that are present in the most recent releases of the X-ray catalogues publicly available. Like we explained in Section 2, since each of them is based on a number of years of observations, we did not include sources that have been detected in observations performed after the time span covered by the catalogue.

We found that among the 48 γ-ray sources only 23 have at least an X-ray counterpart candidate inside the 95 per cent-confidence γ-ray source error ellipse from at least one of the three X-ray surveys (Fig. 1). The results of the cross-matches with the X-ray catalogues for these 23 γ-ray sources are visualized in more detail in Fig. 2 and summarized in columns 3–5 of Table 1. The majority of X-ray candidate counterparts (41) comes from the 3XMM/DR8 catalogue, while 14 come from the 1SXPS and 19 from the CSC 2.0. The relatively small number of X-ray sources detected by each facility is explained both by the random coverage of each γ-ray error ellipse and the random distribution of the X-ray integration times (Fig. 3).

For the γ-ray sources with X-ray coverage from more than one X-ray satellite, we checked how many X-ray candidate counterparts have been detected by more than one satellite. This we did by matching the X-ray source coordinates using a radius of 5 arcsec to account for the absolute astrometry accuracy in the detector focal plane of each X-ray satellite. For *XMM–Newton* the median value is generally 1.5 arcsec,[4] for *Swift* it is 5.5 arcsec (90 per cent confidence; Evans et al. 2013), while for *Chandra* it is 0.8 arcsec
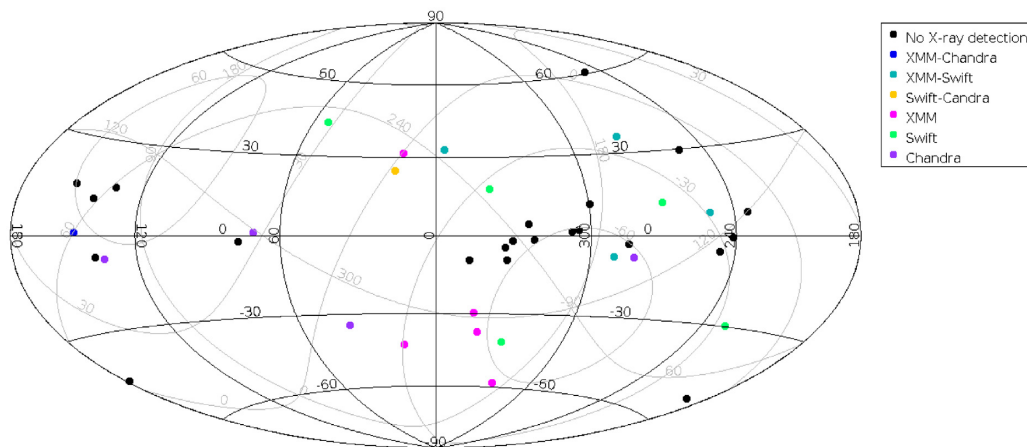
---

[4]Calibration technical note XMM-SOC-CAL-TN-0018.

Figure 1. Sky map in Galactic coordinates (black solid lines) with the positions of the 48 γ-ray MSP candidates of Saz Parkinson et al. (2016) marked with different colours depending on the X-ray coverage from different surveys (see legend). γ-ray sources with no X-ray coverage in any of the reference surveys are plotted in black. As it can be seen, these sources are mostly distributed along the Galactic plane, which may reflect an observational bias in the coverage of these crowded X-ray source regions.

(90 per cent confidence), up to a maximum of 2 arcsec for sources observed at large off-axis angles.[5] The coordinate match implies 64 unique candidate X-ray counterparts across all the 23 γ-ray sources in Table 1.

Of course, given the sparse X-ray coverage of the γ-ray error ellipses (Fig. 2), we cannot rule out that either actual X-ray counterparts to our γ-ray sources are missed in this selection owing to the partial X-ray coverage of the error ellipses of these 23 γ-ray sources or that others lurk among the remaining 25 γ-ray sources with no X-ray coverage at all. In both cases, identifying candidate MSPs without an X-ray footprint by running blind periodicity searches of the several hundred optical sources in each of the γ-ray error ellipses is beyond the goals of this work. These sources will be reconsidered for further investigations whenever adequate X-ray coverage is available.

The time coverage of the γ-ray source error ellipses is also different for the different X-ray catalogues (Fig. 3). In particular, for most *Swift* sources the total exposure time (i.e. integrated over all observations) is below ~ 10 ks whereas for most *Chandra* sources it is below ~ 50 ks. For about half of the *XMM–Newton* sources, however, the exposure time peaks at ~ 140 and ~ 180 ks, whereas for the rest it is mostly below ~ 50 ks, and for about one-third of the *Chandra* sources it exceeds ~ 400 ks. Therefore, apart from the last case, the longest exposures of the γ-ray source fields are achieved for the *XMM–Newton* sources.

Ten of the 23 γ-ray sources in Table 1 have already a confirmed/proposed identification: 4FGL J0359.4+5414 is identified with an isolated young pulsar (PSR J0359+5414; Clark et al. 2017), 4FGL J1946.5−5402 with a binary MSP (PSR J1946−5403; Camilo et al. 2015), 4FGL J1035.4−6720 and 4FGL J1744.0−7618 with isolated MSPs (PSR J1035−6720 and PSR J1744−76194; Clark et al. 2018), and they all have a pulsar association in the 4FGL (see Section 3.1). Furthermore, 4FGL J1544.5−1126 is a candidate transitional MSP (Bogdanov & Halpern 2015), whereas 4FGL J0523.3−2527, 4FGL J0838.7−2827, 4FGL J0955.3−3949, and 4FGL J2039.5−5617 are candidate RBs (Strader et al. 2014; Halpern, Bogdanov & Thorstensen 2017a; Salvetti et al. 2017; Li et al. 2018), and 4FGL J1653.6−0158 is a candidate BW (Romani et al. 2014), where from here on we use the term 'candidate' to refer

to those sources for which the radio/γ-ray pulsation evidence has not been obtained yet. In particular, four of the seven γ-ray sources out of the original 48 in our starting sample which have been classified as pulsars in the 4FGL catalogue (see Section 3.1) are recovered in Table 1 (PSR J0359+5414, PSR J1946 5403, PSR J1035−6720, and PSR J1744−76194). The remaining three (PSR J0318+0253, PSR J1528−5838, and PSR J1641−5317) are not included in Table 1 since they have no X-ray counterpart yet. Indeed, they have all been observed by *Swift* but the exposure time was too short (a few ks) to allow their X-ray detection. PSR J1528−5838 was also observed by *XMM–Newton* on 2019 August 28 with an exposure time of 18.8 ks but the data cannot be obviously included in 3XMM/DR8.

3.3 Cross-correlation with optical catalogues

As a next step, we looked for candidate optical counterparts to the X-ray sources detected in the 23 candidate γ-ray source fields. Among them, we then selected those for which we found evidence of a periodic optical flux modulation of less than 1 d (Section 3.4) since this is the clear signature of the kind of binary systems we are looking for, associated with the tidally distorted and heated companion star surface (Section 2). For each γ-ray source field, we performed the cross-match between the associated X-ray source list and the most recent catalogue release from the four different multi-epoch optical sky surveys discussed in Section 2 (Catalina, PTF, ZTF, PanSTARRS) using a matching radius of 5 arcsec. The choice of a radius of 5 arcsec is justified to account for the accuracy on the absolute coordinates of the X-ray sources (Section 3.2), which dominates over that of the optical catalogues, which is of the order of 0.1–0.5 arcsec. As a safe measure against possible fake detections, we visually verified the matches directly on the optical images.

Out of the 23 γ-ray sources with candidate X-ray counterparts, 17 have also possible optical counterparts to the X-ray sources in at least one of the selected multi-epoch surveys. The results of the cross-match of the X-ray sources detected in the error ellipses of the 17 γ-ray sources with the selected optical catalogues are summarized in the last four columns of Table 1. Like we did for the candidate X-ray counterparts (Section 3.2), we identified candidate optical counterparts detected across different surveys based upon their coordinates. Following our strategy, we will focus our joint
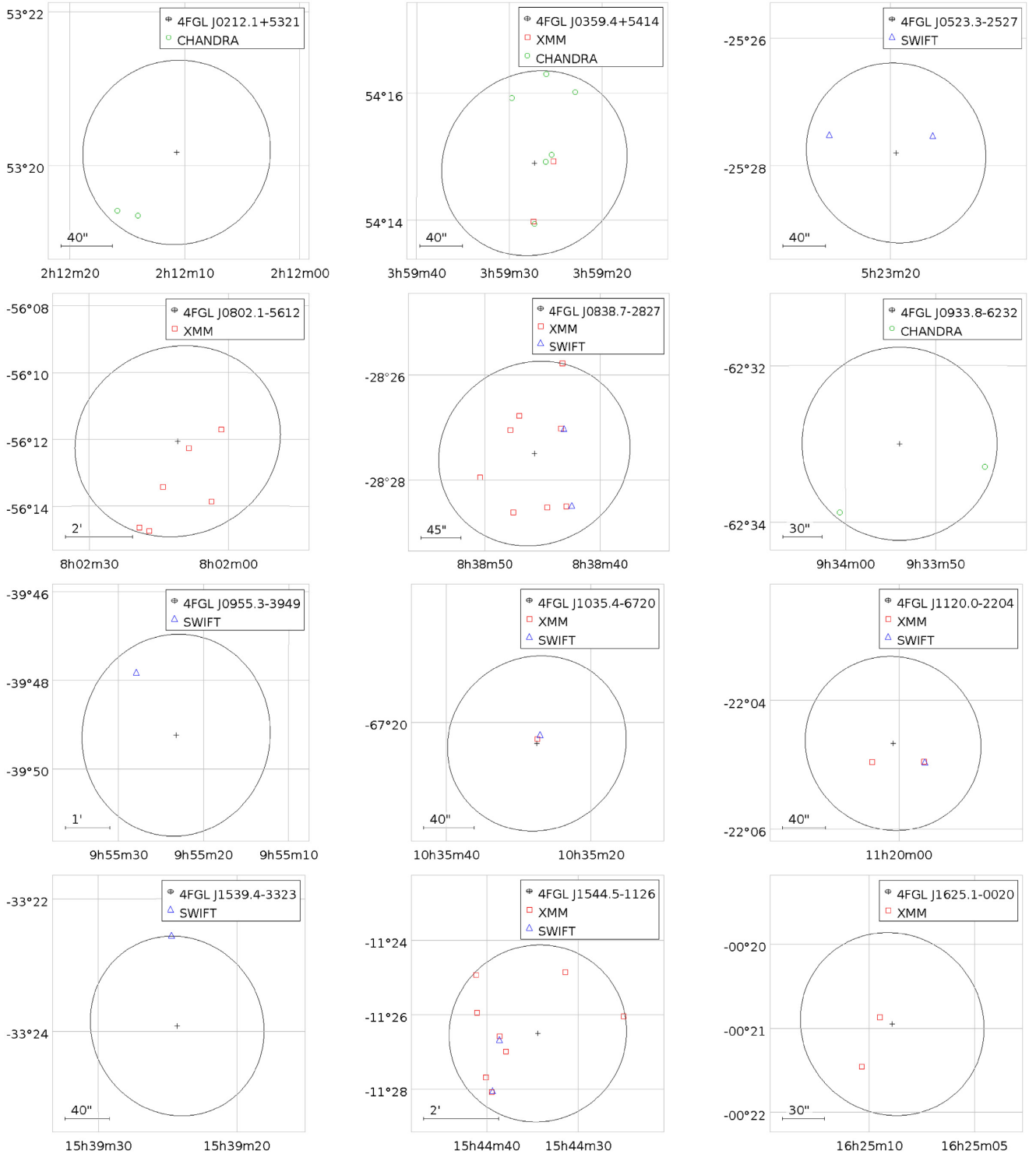
[5]https://cxc.cfa.harvard.edu/cal/ASPECT/celmon/

Figure 2. 4FGL 95 per cent confidence error ellipses of the 23 γ-ray MSP candidates of Saz Parkinson et al. (2016) with X-ray coverage from *XMM–Newton*, *Swift*, or *Chandra*. X-ray sources from the corresponding X-ray catalogues are overplotted and marked with different symbols and colours (see legenda).

X-ray/optical analysis on these 17 γ-ray sources, which passed the second screening and, thus, represent our primary working sample. The search for periodic modulations in the flux of the candidate optical counterparts to these 17 γ-ray sources is presented in Section 3.4.

Similarly to what we discussed in Section 3.2, we are aware of the risk of missing actual X-ray counterparts to our candidate γ-ray sources among the six for which we have no associated optical counterpart. Indeed, their identification based on the search for orbital periodicity on the X-ray data alone is not straightforward given the average duration of the single X-ray observations compared to that of the expected orbital periods and the serendipitous multi-epoch coverage, which for 3XMM/DR8 are $\approx$24 ks and 1–5 epochs, respectively. None the less, also spurred by the case of 3FGL 2039.6−5618
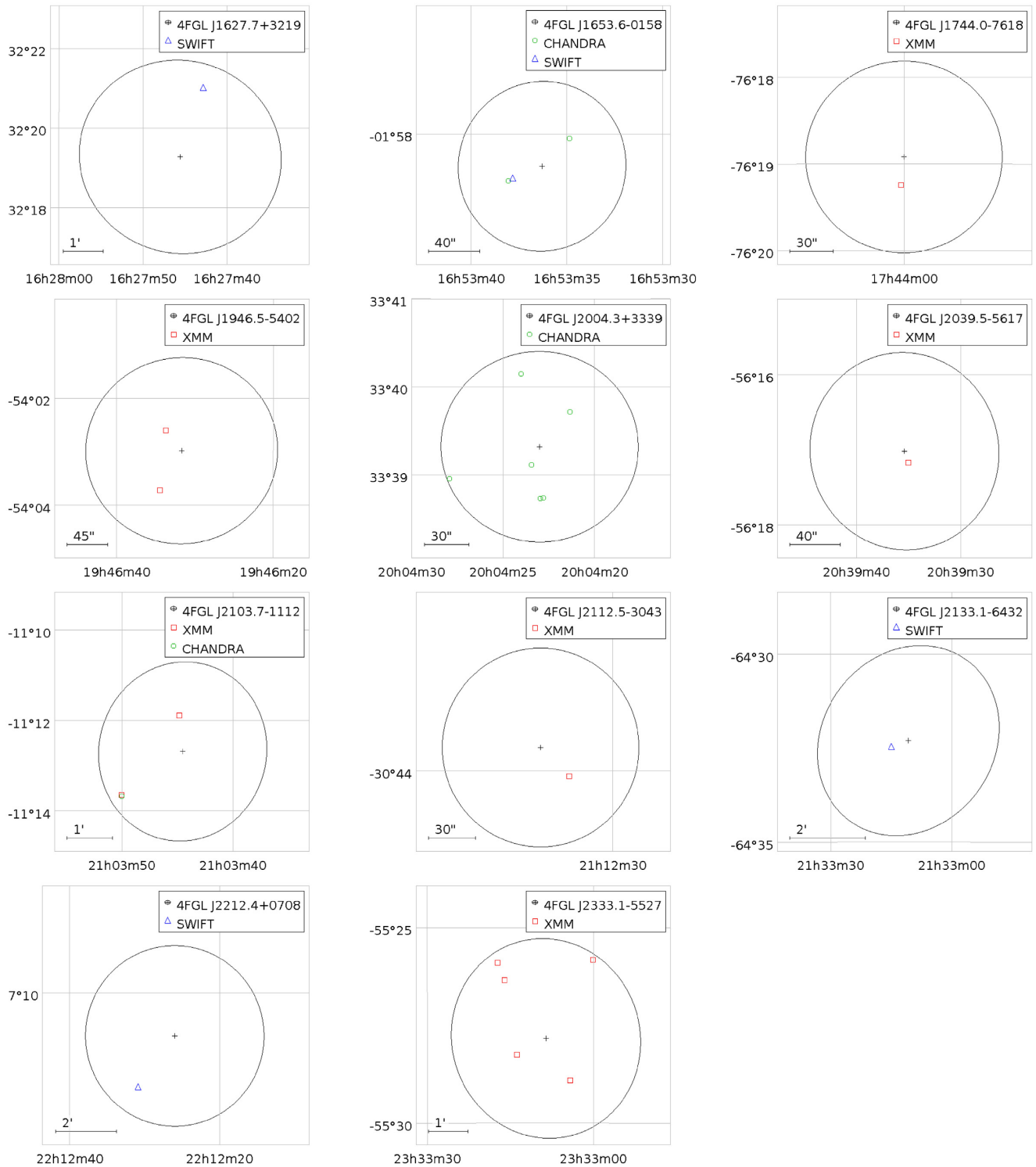
Figure 2. Continued.

for which the orbital periodicity was first discovered in the X-rays (Salvetti et al. 2015), we carried out a periodicity search for all the candidate X-ray counterparts associated with these six γ-ray sources, as well as for those associated with the 17 γ-ray sources that have candidate optical counterparts (see Section 3.5). We note that a direct search for X-ray pulsations is not possible since the observations the X-ray catalogues are built upon have not been acquired in timing mode, hence they have no adequate time resolution for periodicity searches on ms time scales.

3.4 Optical periodicity analysis

To search for an orbital periodicity of the candidate optical counterparts we used an off-line computation tool based on the

Table 1. Summary of the results of the multiwavelength cross-correlations of the 48 γ-ray MSP candidates selected in Section 2. Those with an least a candidate X-ray counterpart are 23, of which 17 have an associated optical counterpart. Columns identify the 4FGL name of the γ-ray source, the source identification, for the 10 sources for which it is available, as isolated young pulsar (iPSR), isolated MSP (iMSP), candidate transitional MSP (ctMSP), binary MSP (bMSP), candidate BW or RB (cBW/cRB), the candidate X-ray counterparts in the selected X-ray catalogues (3XMM, 1SXPS, 2CXO), and their associated optical counterparts in the multi-epoch surveys (Catalina, PTF, ZTF, PanSTARRS), if any. In the PanSTARRS catalogue, the same object can appear with multiple IDs corresponding to its detection in different observations. For the sake of clarity and compactness, we only show one ID for each object. Optical counterparts with a confirmed/candidate periodicity (P) are marked by the superscript. The MSP candidates studied in Salvetti et al. (2017) are marked by the asterisk.

4FGL	Id.	3XMM	1SXPS	2CXO	CSS	PTF	ZTF	PanSTARRS
J0212.1+5321	–	–	–	J021214.0+531920	–	–	7762083000032329	–
				J021215.8+531924			7752054000044594	–
J0359.4+5414	iPSR	J035925.2+541455		J035926.0+541455			778207100035977	–
				J035925.4+541501			778207100048011	–
				J035922.8+541601				–
		J035927.3+541358		J035927.2+541356		48822060004599	778107100010205	173110598739469282
				J035929.7+541555				–
				J035926.0+541618				–
J0523.3−2527*	cRB		J052317.0−252732		J052316.9−252737^P		256107300002741	77440808205337977
			J052324.2−252732		J052324.4−252731		256207300002270	77440808516949749
J0802.1−5612*	–	J080203.6−561352			J080203.6−561354			–
		J080217.0−561444			J080216.8−561444			–
		J080201.5−561142						–
		J080208.5−561216						–
		J080214.0−561325						–
		J080219.2−561438						–
J0838.7−2827	cRB	J083842.9−282830	J083842.4−282830					73812967829839968
		J083843.2−282546						
		J083843.3−282701	J083843.1−282702					
		J083844.5−282831						
		J083846.9−282646						73851296805669950
		J083847.7−282702						73831296857810040
		J083850.4−282757						73861296944754027
		J083847.5−282837						73841297100561268
J0933.8−6232	–			J093344.5−623317				–
				J093400.6−623352				–
J0955.3−3949	cRB		J095527.8−394750		J095527.8−394752^P			–
J1035.4−6720*	iMSP	J103527.3−672013	J103526.9−672010					
J1120.0−2204*		J111958.3−220456	J111958.2−220458		J111958.3−220456		2681154000002304	81501699903115522
		J112001.7−220457			J112001.7−220457		2682154000011285	81501700074071334
J1539.4−3323*		–	J153924.7−332233					
J1544.5−1126	ctMSP	J154425.0−112602						
		J154431.4−112451				22137209010448		94302361306503089
		J154437.8−112659						
		J154438.5−112634	J154438.5−112641		J154438.5−112641	22137209010841	3782084000009125	94262361606388530
		J154439.4−112804	J154439.3−112804		J154439.4−112804		3781084000011640	94232361604998794
		J154440.0−112741				22137209010994	3782084000009349	94242361661476451
		J154441.0−112557						
		J154441.1−112456					3782084000008746	94302361717401469

Table 1 *– continued*

4FGL	Id.	3XMM	1SXPS	2CXO	CSS	PTF	ZTF	PanSTARRS
J1625.1−0020*	−	J162509.4−002052	−	−	J162509.5−002051	−	−	−
		J162510.3−002127						−
J1627.7+3219	−	−	J162742.8+322059	−	J162743.0+322103[P]	41621060004671[P]	679105100004944	146822469291741697
J1653.6−0158*	cBW	J165337.8−015835		J165338.0−015836	J165338.1−015836[P]	26652110004413	432112400014707	105622534086488129
		−		J165334.8−015803	−	26652115002981	−	105632533941618183
J1744.0−7618*	iMSP	J174400.6−761914						−
J1946.5−5402	bMSP[a]	J194633.6−540236			J194633.7−540236			−
		J194634.4−540343						
J2004.3+3339	−	−		J200421.3+333942			688209300101711	148393010879214642
							688209300084182	148393010887423147
		−		J200422.7+333844			686109300049900	148373010937876456
							688209300122014	148373010954324969
		−		J200422.9+333843			688209300122014	148373010954324969
		−		J200423.4+333906			686209300131114	148383010978953660
							686109300072405	148383010985852102
							686109300089082	148383010967343943
		−		J200424.0+334008	−		688209300032950	148440301000363517
		−		J200427.9+333857	−		686209300128511	148373011155519463
							688209300033911	148383011165801287
J2039.5−5617*	cRB	J203935.0−561710	−	−	J203934.9−561708[P]	−	−	−
J2103.7−1112	−	J210344.8−111153	−	−		−	−	94563159378063313
		J210350.0−111338	−	J210350.0−111341	J210350.1−111341	2264207000000705	389106300020270	945215958696916709
J2112.5−3043*	−	J211232.1−304403	−	−	−	−	−	−
J2133.1−6432	−		J213314.9−643229					−
J2212.4+0708	−	−	J221230.8+070651	−	J221231.0+070652[P]	31092070002977	494213400002994	116533331290607966
J2333.1−5527	−	J233300.1−552549	−	−	−	−	−	−
		J233304.1−552854	−	−	−	−	−	−
		J233313.8−552814	−	−		−	−	−
		J233316.0−552620	−	−	J233315.9−552620	−	−	−
		J233317.3−552554	−	−		−	−	−

[a] 4FGL J1946.5−5402 is identified with a binary MSP (PSR J1946−5403) which is considered a possible BW candidate (Camilo et al. 2015).
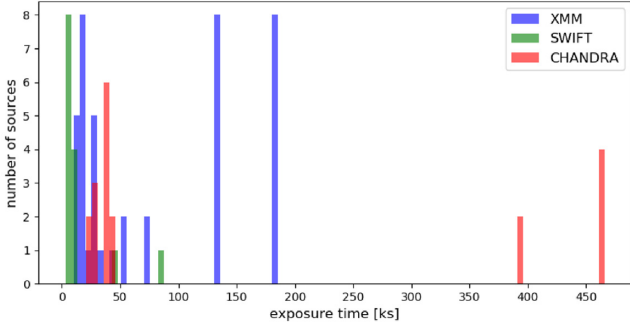
Figure 3. Histogram of the total integration time for all sources detected by *XMM–Newton* (41), *Swift* (14), and *Chandra* (19) in the error ellipses of the 23 γ-ray sources with X-ray coverage (Table 1).

Lomb–Scargle (LS) periodogram algorithm. Since the data for most of the candidate optical counterparts are unevenly-sampled in time, the LS periodogram is a suitable algorithm to use. We used the ASTROPY implementation of the LS algorithm, which is based on the code presented in VanderPlas et al. (2012) and VanderPlas & Ivezić (2015). In each periodogram, we computed the peak significance level following a procedure similar to that explained in the work of Süveges (2014). This is based on the combination of both non-parametric bootstrap resampling, which allows one to reproduce the empirical distribution of the periodogram peaks, and extreme-value models which provide asymptotically valid models for the tails of more continuous distributions. For each optical candidate counterpart, we created 1000 bootstrap repetitions of the original time series extracted from the multi-epoch sky surveys preserving the epochs of observation and replacing the object magnitudes in each observation with values randomly chosen with equal probabilities from the original data set. For each bootstrap we computed the corresponding periodogram and extracted the highest peak. The empirical distribution of the highest peaks obtained from the bootstrap was modelled on a generalized extreme-value distribution from which we computed the level corresponding to a false alarm probability of 0.01 (99 per cent significance threshold). Only peaks above this significance threshold were associated with a candidate periodicity in the time series. In our analysis of the LS periodograms we carefully verified the presence of spurious peaks that could be attributed to aliases caused by the cadence of the observations when taken at ≈1 d/cycles and around the same time in the night.

Among the 23 γ-ray sources with possible X-ray counterparts only 17 had at least one of the X-ray sources with an associated optical counterpart (Section 3.3). Among them, only seven confirmed/candidate γ-ray MSPs show evidence of orbital periodicity in at least one of their associated optical counterparts from the survey data. The results are summarized in Table 2, where we report the associated optical counterparts from the different surveys and the computed period. Four of these MSP candidates have already been classified as actual binary MSPs (BWs/RBs or other types) in previous studies and the orbital periods measured from their optical counterparts are reported in the literature, with our results in agreement with them. Like we already stated in Section 3.1, we did not exclude these sources from our optical periodicity analysis because they provide an essential test to establish the validity of our method and to ensure the reliability of the results obtained for the remaining three γ-ray MSP candidates which have not been identified yet.

Table 2. Summary of the confirmed/candidate γ-ray MSPs listed in Table 1 with either known or candidate orbital periodicity. X-ray counterparts are listed in columns 3–5. Sources for which the companion star has been optically identified from previous works are marked by the superscript PB and has been measured in the optical, either from photometry or spectroscopy measurements. The values of the orbital period computed in this work from the LS periodogram analysis of the optical light curves from the survey data (columns 6 and 7) are listed in the column 9 together with the associated uncertainties. The computed significance of the corresponding periodogram peak is listed in the last column. Periods in agreement with values reported in the literature are marked in bold and candidate periods in italics. Orbital periods that we could not recover through our LS periodogram analysis are marked in roman. For 4FGL J0838.7−2827 and 4FGL J1544.5−1126 the orbital period has been measured from optical photometry and spectroscopy, respectively, whereas for 4FGL J1946.5−5402 (PSR J1946−5403) from radio timing observations.

4FGL	Id.	3XMM	1SXPS	2CXO	Catalina	PTF	(V)	Period (d)	Significance
J0523.3−2527[O,PB]	cRB[1]	–	J052317.0−252732	–	J052316.9−252737		16.51	**0.68813(6)**	7σ
J0838.7−2827[O,PB]	cRB[2]	J083850.4−282757			–	–			0.214507	
J0955.3−3949[O,PB]	cRB[3]	–	J095527.8−394750	–	J095527.8−394752		18.45	**0.38733(6)**	7σ
J1544.5−1126[O,PB]	ctMSP[4]	J154439.4−112804	J154439.3−112804	–	J154439.4−112804		18.18	0.2415361	
J1627.7+3219	–	–	J162742.8+322059	–	J162743.0+322103	41621060004671	13.35	*0.4992772*	7σ
J1653.6−0158[O,PB]	BW[5]	–	J165337.8−015835	J165338.0−015836	J165338.1−015836		20.26	**0.054799(2)**	7σ
J1946.5−5402	bMSP[6]	J194633.6−540236	–	–	J194633.7−540236		19.31	0.13	
J2039.5−5617[O,PB]	cRB[7]	J203935.0−561710	–	–	J203934.9−561708		18.54	**0.22798(3)**	7σ
J2212.4+0708	–	–	J221230.8+070651	–	J221231.0+070652		19.70	*0.31884(6)*	3.2σ

Note. **References:** (1) Strader et al. (2014); (2) Halpern et al. (2017b); (3) Li et al. (2018); (4) Britt et al. (2017); (5) Romani et al. (2014); (6) Camilo et al. (2015); (7) Salvetti et al. (2015).

The small number of optical counterparts with evidence of orbital periodicity can be naturally explained by observation biases. First, the computation of the orbital periodicity was carried out successfully only for those candidate optical counterparts for which the number of observations was high enough to guarantee a statistically significant set of data for the LS periodogram computation. In particular, we computed the periodogram only for sources with at least 50 observations available. Secondly, not all surveys could be exploited at the same level. For instance, Catalina, PTF, and ZTF explore the sky in one specific optical band, whereas PanSTARRS observes in five different bands and the number of observations per band is uneven. In this case, the criteria for the periodogram computation was to select the band that maximises the number of observations available, which might have ended up not being always adequate. Moreover, the time span covered by the four surveys is different, which means that the number of observations that they have collected over the years is also different. Indeed, for the seven sources with periodically modulated candidate optical counterparts, the period was mainly computed from the Catalina data and only in one case also with the PTF data, even though the same object was detected in more than one survey. This is because Catalina and PTF are the surveys that have been running for the longest time among the four that we used. Finally, even when enough observations were available the survey cadence was not always suitable for the investigation of a periodicity of less than about 1 d.

3.5 X-ray periodicity/variability analysis

Since for both RBs and BWs we expect that the X-ray flux is modulated at the orbital period of the binary system, owing to the emission from the intra-binary shock, we performed a systematic periodicity search in the X-ray data, targeted at periods smaller than 1 d. In principle, one should skip this step for the three γ-ray sources identified as isolated eitheryoung pulsars or isolated MSPs, i.e. 4FGL J0359.4+5414, 4FGL J1035.4−6720, 4FGL J1744.0−7618 (Table 1). In these cases, however, an eventual chance coincidence with a periodically modulated X-ray source would help to assess the validity of this method to identify candidate BWs and RBs. We focused our periodicity analysis on the *XMM–Newton* data, which provide most of the X-ray candidate identifications (Section 3.2). Furthermore, for the analysis of these data we could capitalise on the automatic tools developed within the *EXTraS* project[6] (De Luca et al. 2016). There are 41 X-ray sources in 3XMM/DR8 associated with 13 γ-ray sources (Table 1), including those with or without a likely optical counterpart, and we carried out the periodicity analysis for all of them.

At the same time, we carried out a general search for long-term X-ray flux variability in the *XMM–Newton* data, which might reflect the transition from rotation-powered to accretion-powered states, like in transitional MSPs. Finally, since RBs also feature flaring activity (Halpern et al. 2017a) we also looked for X-ray flares in the *XMM–Newton* observations of our γ-ray sources. Depending on the flare duration and intensity and on the persistent flux level, sources of X-ray flares can be detected only in some parts of an observation and might not appear in the 3XMM/DR8 catalogue, where the source detection is run on the whole time-integrated observation. Therefore, such sources might not be listed in Table 1. In both cases, we used the tools specifically developed within the *EXTraS* projects.

[6]http://www.extras-fp7.eu/

4 DISCUSSION OF RESULTS

Starting from the sample of the 48 γ-ray MSP candidates of Saz Parkinson et al. (2016), out of the 23 with possible X-ray counterparts we extracted 17 γ-ray sources with associated optical counterparts (Table 1), of which only six feature a more or less clear evidence of orbital periodicity (Table 2) according to our LS periodogram analysis. Apart from the observational biases described in Section 3.4, such a small number can also be explained by the intrinsically non-homogeneous nature of our sample. Indeed, the 48 γ-ray MSP candidates of Saz Parkinson et al. (2016) in principle include both isolated and binary MSPs, as discussed in Section 2. In the first place, we do not expect to observe isolated MSPs since neutron stars are very faint objects in the optical (Mignani 2011), far below the limiting magnitudes of the optical surveys used in this work which are in the range 22–23. Furthermore, most binary MSPs have WD companions. Because of their compactness, WDs are less subject to tidal distortion and less affected by irradiation from the MSP. Therefore, they are not expected to exhibit significant modulations of the optical flux along the binary system orbit. In conclusion, the restricted class of RBs/BWs remains the only promising target for our periodicity search.

The results of our optical variability analysis for known and candidate BWs/RBs are discussed on a case by case basis in Sections 4.1 and 4.2, respectively. The status of proposed but yet unconfirmed BW/RB identifications for which we could not find either an optical counterpart or an optical periodicity is updated in Section 4.3. Finally, the discussion of the results of our multiwavelength variability analysis is supplemented in Section 4.4 that is focused on the X-ray observations.

4.1 Known BW/RB candidates

Out of the six known BW/RB and tMSP candidates (Table 1), we could recover orbital periodicity of the optical counterparts only for the three RB candidates 4FGL J0523.3−2527, 4FGL J0955.3−3949, 4FGL J2039.5−5617 and for the BW 4FGL J1653.6−0158. For the candidate tMSP 4FGL J1544.5−1126, we could not find a periodicity in agreement with the published value, whereas for the remaining known RB candidate 4FGL J0838.7−2827 the available optical survey data did not allow us to run a periodicity search. For the binary MSP 4FGL J1946.5−5402, which is a possible BW candidate, the periodicity search did not provide convincing evidence of flux modulations at the known orbital period.

4.1.1 4FGL J0523.3−2527

4FGL J0523.3−2527 is a candidate RB with orbital period $P_B = 0.688\,134(28)$ d measured in the optical (Strader et al. 2014). We found optical coverage with the Catalina (CSS and SSS), ZTF, and PanSTARRS surveys but, due to the scarcity of observations in both ZTF and PanSTARRS, only the Catalina data allowed us to run the periodicity search. The companion star of the RB candidate 4FGL J0523.3−2527 is detected in both the CSS and SSS (CSS/SSS J052316.9−252737). After combining the data collected by both surveys, we obtained a sample of 244 observations from which we found a period of 0.688 13 d in the LS periodogram. The corresponding folded light curve is shown in Fig. 4, which is in agreement with that originally measured by Strader et al. (2014) also from the CSS/SSS data and already confirmed by Salvetti et al. (2015). We also find an alias at half the above reported period in the periodogram. This was also found in the analysis of
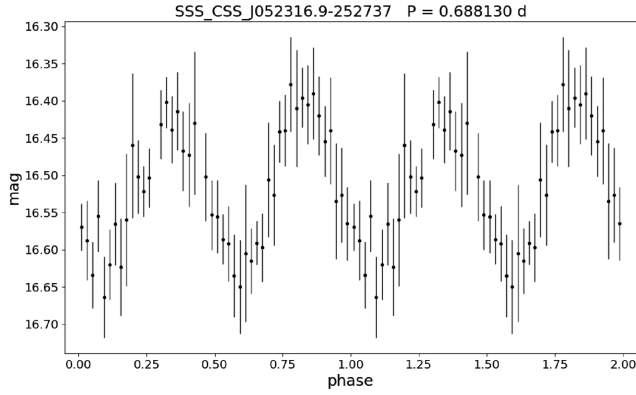
Figure 4. Two clear peaks are recognized in the LS periodogram at periods of 0.344 065 d and its double 0.688 13 d. Folded Catalina light curve at the longer period, which has been confirmed by optical spectroscopy (Strader et al. 2014). Two cycles are shown for clarity. A rebin of a factor of 5 in phase has been applied after rejection of outlier photometry measurements to better show the light-curve morphology. Two slightly asymmetric maxima separated in phase by ∼0.5 are clearly recognized, as shown by Strader et al. (2014). The absolute phase of the folded light curve is set arbitrarily.

Strader et al. (2014) and ruled out as the actual period of the binary system because it was in disagreement with the value measured independently from the radial velocity curve obtained from optical spectroscopy.

4.1.2 4FGL J0838.7−2827

Another of the known RB candidates with a likely optical counterpart in our survey data is 4FGL J0838.7−2827. This source was previously studied in the work of Rea et al. (2017) where they proposed a few X-ray candidate counterparts possibly associated with the γ-ray source. One of them, 3XMM J083850.4−282757, shows variable X-ray emission, with a powerful flare (Halpern et al. 2017a) similar to those observed in transitional MSPs during the sub-luminous disc state. For this reason, it is considered the most likely X-ray counterpart to 4FGL J0838.7−2827 also based upon the detection of an ∼0.21 d optical flux modulation (Halpern, Strader & Li 2017b). For this X-ray source we found an associated optical counterpart in PanSTARRS only, but the scarcity of observations did not allow us to run the periodicity search and independently confirm the detection of the ∼0.21 d optical flux modulation (Halpern et al. 2017b). Folding the PanSTARRS data around this period does not produce evidence of periodic modulations in the light curve and is not shown here.

4.1.3 4FGL J0955.3−3949

4FGL J0955.3−3949 is a candidate RB with an orbital period $P_B = 0.387 3318(13)$ d, discovered from a period search at the position of its *Swift* candidate X-ray counterpart (1SXPS J165337.8−01583) using the Catalina data (Li et al. 2018). In this work, we recovered the X-ray source association with the same Catalina source (SSS 095527.8−394752), not detected in PTF, ZTF, and PannSTARRS, and independently searched for periodicity. We detected a main peak in the LS periodogram at a period of 0.387 33(6) d, which is in very good agreement with the results of Li et al. (2018). The corresponding folded light curve is shown in (Fig. 5).
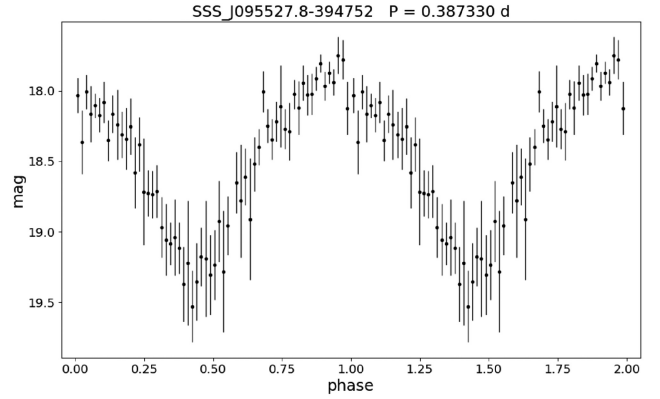
Figure 5. Catalina light curve computed from the Catalina data of the companion star to the RB candidate 4FGL J0955.3−3949 folded at the period of the LS periodogram main peak, 0.387 33(6) d, after rebinning by a factor of 3. A single broad maximum is apparent, consistent with the light curve published in Li et al. (2018).
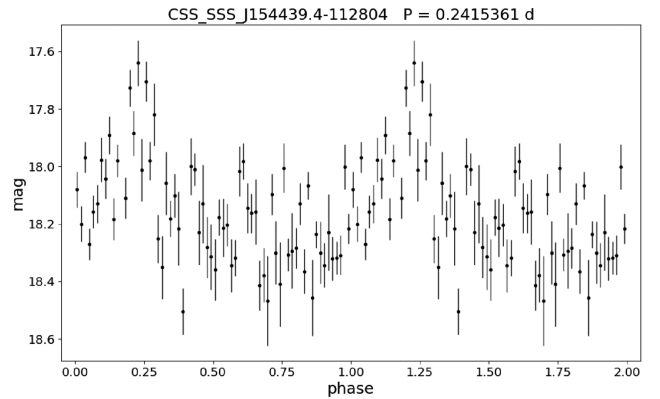

Figure 6. Catalina light curve of the companion star to 4FGL J1544.5−1126 (CSS, SSS J154439.4−112804) folded at the orbital period $P_{orb} = 0.241 5361(36)$ d measured from the radial velocity curve (Britt et al. 2017). A rebinning by a factor of 5 in phase has been applied for a better visualization.

4.1.4 4FGL J1544.5−1126

4FGL J1544.5−1126 is a candidate transitional MSP. Radial velocity measurements obtained from optical spectroscopy of the companion star (Britt et al. 2017) showed that this is a remarkably face-on binary system with inclination $i = 5°$–$8°$ and an orbital period $P_B = 0.241 5361(36)$ d. Previous studies of the companion star light curve failed to detect a clear periodic flux modulation (Bogdanov & Halpern 2015). We found optical coverage from Catalina, ZTF, and PanSTARRS but only for Catalina the number of observations was adequate for the periodogram computation. Both by combining the observations of the three surveys (CSS, MLS, SSS) and analysing them separately we could not find a peak in the LS periodogram corresponding to the known orbital period. We also folded the Catalina data at the period measured by Britt et al. (2017) but, while one can recognise a possible flux modulation with a single broad maximum (Fig. 6), it is not clear whether this is ascribed to a genuine orbital variability or to the folding of data affected by short-term variability characterised by a sequence of minima and maxima occurring on few hour time-scales (Bogdanov & Halpern 2015). This trend cannot be recognised in the unfolded Catalina light curve owing
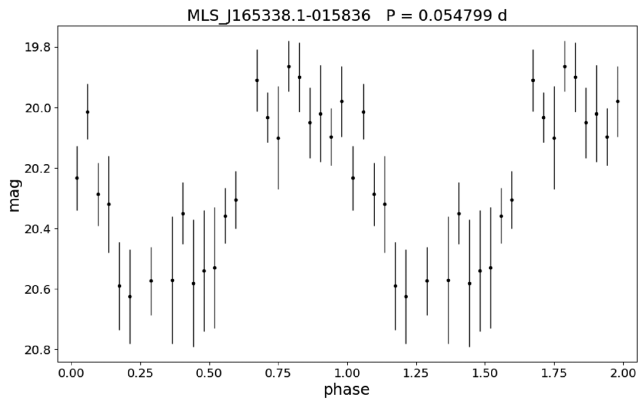
Figure 7. Catalina light curve from the Catalina data of the companion star to the BW candidate 4FGL J1653.6−0158 folded at the period of the periodogram main peak, 0.054 799(2) d, after rebinning by a factor of 2. A single broad maximum is apparent, consistent with the light curve published in Romani et al. (2014).

to the coarser data sampling. Catalina data spanning 7 yr were also analysed by Bogdanov & Halpern (2015) who concluded that there was no significant evidence of a modulation. Future observations should restrict the periodicity search to time intervals selected to avoid the light curve minima and maxima.

4.1.5 4FGL J1653.6−0158

4FGL J1653.6−0158 is a candidate BW with the shortest orbital period known of $P_B = 0.0519 4469(+10, -08)$ d measured by Romani et al. (2014) and obtained by combining SOAR, WIYN, and Catalina (MLS) observations of the optical counterpart. This was also studied by Salvetti et al. (2017) using the Catalina data alone and the periodicity was confirmed. We detected the optical counterpart to 4FGL J1653.6−0158 in all the optical surveys considered in this work but only for Catalina the number of observations allowed us to run the periodicity search. We found a peak in the periodogram at a period of 0.054 799(2) d, with the folded light curve shown in Fig. 7. The period value not in complete agreement with the value obtained by Romani et al. (2014) but is consistent with that independently obtained by Salvetti et al. (2017) using the same Catalina data (0.054 798 941 02 d). The difference in the period determinations is probably ascribed to the sparse data and large error bars of the Catalina data with respect to the combined data set used by Romani et al. (2014), which makes the period computation less precise.

4.1.6 4FGL J1946.5−5402

4FGL J1946.5−5402 is identified with the binary MSP PSR J1946−5403 discovered in a Parkes radio search by Camilo et al. (2015) at a DM-derived distance of ∼1.15 kc (Yao, Manchester & Wang 2017). The system has an a orbital period of $P_B = 0.130$ d and, based on the lower limit on the companion star mass ($M_C \gtrsim 0.021 \, M_\odot$), is considered a candidate BW although no radio eclipses have been detected yet. Owing to the large uncertainty of ∼7 arcmin associated with the radio position (Camilo et al. 2015), the companion star to this BW has not been identified yet and no optical periodicity has been found. In our work we only found an object in Catalina (SSS J194633.7−540236; $V = 19.31$), at a position consistent with the coordinates of 3XMM J194633.6−540236, one of the two X-ray
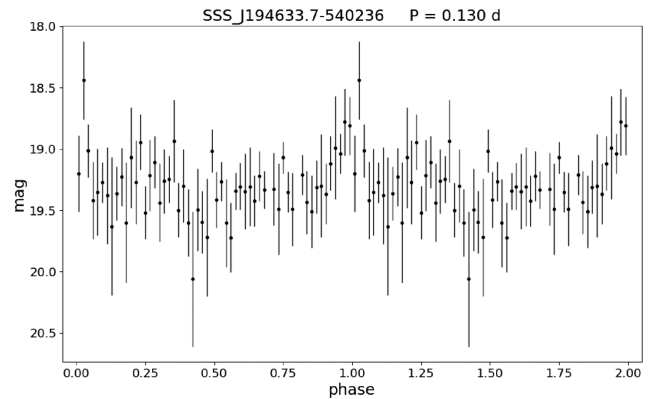

Figure 8. Catalina light curve of SSS J194633.7−540236 folded at the orbital period (0.130 d) of PSR J1946−5403 measured in radio by Camilo et al. (2015). A rebinning by a factor of 5 in phase has been applied for a better visualization.

sources detected in the γ-ray error ellipse of 4FGL J1946.5−5402 (Fig. 2). The X-ray source coordinates are within the radio position uncertainty region of PSR J1946−5403, which makes it a possible X-ray counterpart to the pulsar. Owing to the large error bars in the Catalina data of SSS J194633.7−540236, the periodogram did not reveal any significant peak at a period consistent with that of the PSR J1946−5403 orbit (0.130 d). Folding the Catalina data around this value (Fig. 8) only reveals a weak evidence of modulation which should be investigated through future observations. Therefore, based on the optical data alone we cannot claim an association of 3XMM JJ194633.6−540236/SSS J194633.7−540236 with the pulsar, whose companion star still remains unidentified. An improvement of the pulsar radio position and a better determination of the binary period would help the identification process.

4.1.7 4FGL J2039.5−5617

4FGL J2039.5−5617 is a candidate RB discovered by Salvetti et al. (2015) and Romani (2015) for which they observed an orbital modulation in both X-rays and the optical. Using GROND data they found a period of 0.227 48(43) d that coincides, within the errors, with that of the X-ray source. In this work, we found that the source was observed only by Catalina (SSS J203934.9−561708), which now provides a more extended epoch coverage (223 epochs) than available at the time when Romani (2015) and Salvetti et al. (2017) carried out their periodicity search in the Catalina data. For the first time, we now found that a periodic flux modulation is also detectable in the Catalina data, at a period of 0.227 98(3) d consistent with the value of the orbital period of 0.227 9817(7) d obtained from radial velocity measurements by Strader et al. (2019). As expected, the folded Catalina light curve (Fig. 9) is characterized by two asymmetric maxima separated in phase by ∼0.5, which are less clearly resolved in the more noisy Catalina data. For this reason, we could not find significant evidence of light curve evolution between the epochs of the GROND and Catalina data.

4.2 New BW/RB candidates

The broad agreement between our measured periods and those reported in the literature for four out of the six cases described in the previous section confirms the reliability of our procedure. We now
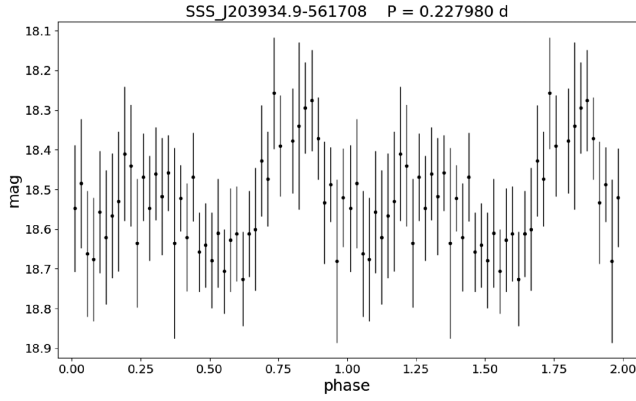
Figure 9. Catalina light curve of the RB candidate 4FGL J2039.5−5617 (Salvetti et al. 2015) folded at the LS peak period of 0.227 98(3) d, which we measured in the Catalina data for the first time, after applying a phase rebinning by a factor of 5. Two asymmetric maxima separated in phase by ∼0.5 are clearly recognized, consistent with what observed in the better signal-to-noise optical light curve obtained from the GROND data (Salvetti et al. 2015).

applied it in the search for new BWs/RBs among the 10 candidate γ-ray MSPs with associated X-ray/optical counterparts (Table 1), for which we searched for a possible optical periodicity for the first time. In particular, there are two candidate γ-ray MSPs in our sample, 4FGL J1627.7+3219 and 4FGL J2212.4+0708, that show peaks in the LS periodogram, which are above the significance threshold and correspond to periods in the range expected for BWs/RBs. We investigate the candidate optical periodicity of these two sources in the following sections. For all the remaining eight candidate γ-ray MSPs with an associated optical counterpart (Table 1), we found either no significant peak in the LS periodogram or we had not enough flux measurements in any of the reference optical surveys for the periodicity search.

4.2.1 *4FGL J1627.7+3219*

For this candidate γ-ray MSP, we found a possible X-ray counterpart detected by *Swift* (1SXPS J162742.8+322059) and an associated, quite bright (V = 13.51), optical counterpart in each of the reference optical surveys. If this object were indeed the companion star in a BW/RB system, the comparison with the optical properties of other BWs/RBs would presumably put it a distance of the order of a few hundred pc. The 4FGL J1627.7+3219 0.1 − 100 GeV energy flux is $(3.3613 \pm 0.35810) \times 10^{-12}$ er g cm^{-2} s^{-1} which, for a distance of 500 pc, would correspond to a γ-ray luminosity of ∼10^{32} erg s^{-1}. This value is within the γ-ray luminosity range of all MSPs but a factor of 10–100 below that of BWs/RBs (Hui & Li 2019). This would imply a correspondingly larger distance for 4FGL J1627.7+3219, if it were indeed a BW/RB, and would argue against the association with its V = 13.51 candidate optical counterpart. That said, we investigated a possible association. Only in PTF and Catalina the number of observations was adequate to run the periodicity search. The LS periodogram computed from the Catalina data show a main peak at a period of 0.499 27(2) d with a significance of 7σ. From the periodicity analysis of PTF data, we found a main peak at a period 0.4991(3) d, similar to that found with Catalina data, with a significance of 4.2σ. Folding the Catalina and PTF light curves at the corresponding peak periods gives very similar profiles, with a single broad maximum (Fig. 10).

4.2.2 *4FGL J2212.4+0708*

This candidate MSP has only one X-ray counterpart found with *Swift* (1SXPS J221230.8+070651) and it is associated with an optical counterpart for which we found a possible periodic modulation. This object (V = 19.7) has been detected by all the four reference optical surveys (Table 1) but, also in this case, only the data collected by Catalina cover a range of epochs large enough to allow the LS periodogram computation. We found a possible period at 0.318 84(6) d, corresponding to the main peak in the LS periodogram, which, however, is only slightly above the computed significance threshold. We folded the Catalina light curve at this period applying a rebinning of a factor five in phase. The folded optical light curve (Fig. 11) shows a possible modulation with two asymmetric maxima, as observed in most RB systems. However, the low significance of the peak in the periodogram makes it difficult to determine whether this periodicity is real. Therefore, we cannot confidently affirm that 4FGL J2212.4+0708 is a RB candidate, although the candidate periodicity is worth investigation through follow-up observations.

4.3 Unconfirmed BW/RB candidates

Five of the unclassified sources in Table 1 (4FGL J0802.1−5612, 4FGL J1120.0−2204, 4FGL J1539.4−3323, 4FGL J1625.1−0020, 4FGL J2112.5−3043) have been previously studied in the optical by Salvetti et al. (2017) using both Catalina and dedicated GROND observations and for one of them (4FGL J0802.1−5612) an orbital periodicity (0.4159 d) was proposed based on the Catalina data. Here, we extended their analysis by adding observations from the PTF, ZTF, and PanSTARRS surveys, with the aim of confirming the proposed periodicity for 4FGL J0802.1−5612 and discovering a candidate periodicity for the other two sources.

4.3.1 *4FGL J0802.1−5612*

The candidate optical counterpart to 4FGL J0802.1−5612 by Salvetti et al. (2017) is SSS J080225.1−560543, associated with the X-ray source 3XMM J080225.3−560542, identified with their field source #5. However, this candidate counterpart now falls clearly outside the revised 4FGL γ-ray error ellipse[7] (Fig. 12) so that we cannot claim an association with 4FGL J0802.1−5612 any longer. For this reason, we did not investigate the SSS J080225.1−560543 variability in other multi-epoch optical surveys. None of the optical counterparts associated with the *XMM–Newton* candidate counterparts to 4FGL J0802.1−5612 (Table 1) show evidence of variability in the Catalina data. Therefore, the identification of 4FGL J0802.1−5612 as a binary MSP remains unconfirmed.

4.3.2 *4FGL J1120.0−2204, 4FGL J1539.4−3323, 4FGL J1625.1−0020, 4FGL J2112.5−3043*

The difference between the 3FGL and 4FGL γ-ray error ellipses for 4FGL J1120.0−2204, 4FGL J1539.4−3323, 4FGL J1625.1−0020, 4FGL J2112.5−3043 is shown in Fig. 12. For 4FGL J1120.0−2204, the new γ-ray error ellipse lies within the 3FGL one and no new candidate X-ray counterparts are found in the *XMM–Newton* data with respect to Salvetti et al. (2017). The optical periodicity of the two current candidate X-ray counterparts 3XMM J111958.3−22045

---

[7]In their work, Salvetti et al. (2017) assumed the, back-then, most recent 3FGL coordinates as a reference.
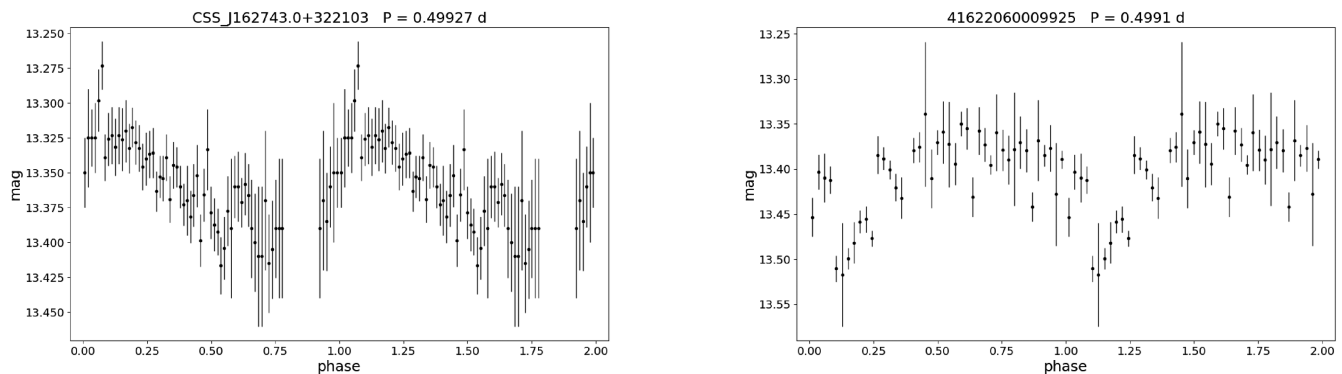
Figure 10. Light curves of the candidate optical counterpart to 4FGL J1627.7+3219 computed from the Catalina (left) and PTF (right) data folded at the main peak periods found in the LS periodograms, 0.499 27(2) and 0.499 1(3) d, respectively. A rebin by a factor of 3 and 4, respectively has been applied.
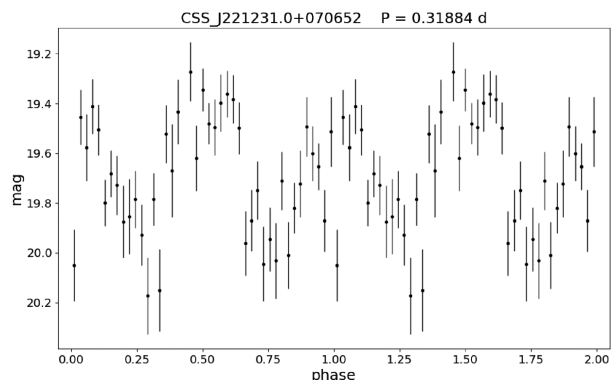

Figure 11. Folded light curve computed from the Catalina data of the BW/RB candidate 4FGL J2212.4+0708 at the LS periodogram main peak of 0.318 84(6) d.

and 3XMM J112001.7−2204 (Table 1), coincident with sources #1 and #2 of Salvetti et al. (2017), have been searched by these authors using Catalina and GROND data but no evidence thereof was found. We re-ran the search in the Catalina as well as the ZTF and PanSTARRS data but, again, we found no evidence of optical periodicity. For 4FGL J1539.4−3323, we found now a candidate *Swift* X-ray counterpart (1SXPS J153924.7−332233), whereas for 4FGL J2112.5−3043 we now found only a candidate *XMM–Newton* counterpart (3XMM J211232.1−304403) identified with field source #1 of Salvetti et al. (2017). In both cases, however, we found no associated optical counterpart in any of the reference surveys. 4FGL J1625.1−0020 has two candidate X-ray counterparts (3XMM J162509.4−002052 and 3XMM J162510.3−002127), identified with field sources #2 and #1 of Salvetti et al. (2017), respectively. They both have potential PanSTARRS associations and the former has also a Catalina association, already investigated in Salvetti et al. (2017), which, however, show no corresponding optical modulation. Therefore, the MSP identification for these four γ-ray sources remains unconfirmed, too.

4.3.3 4FGL J0744.0−2525

Another MSP candidate in the list of Saz Parkinson et al. (2016) for which an optical counterpart was proposed by Salvetti et al. (2017) based upon a clear periodic modulation (0.115 d) detected in the GROND data is 4FGL J0744.0−2525. This RB candidate does not appear in Table 1 because our cross-correlations could not find

an associated X-ray counterpart within the updated 4FGL γ-ray error ellipse, which is only covered by *Swift* observations (Salvetti et al. 2017). Regardless of that, having an optical identification being proposed an independent assessment is in order. We found that the candidate GROND counterpart now falls ∼15 arcsec away from the ∼16-arcsec-wide 4FGL γ-ray error ellipse (Fig. 12), which makes the association somewhat less likely, although not strictly incompatible accounting for possible unknown systematics in the 4FGL position determination. Therefore, we followed up on the proposed optical identification with the PTF, ZTF, and PanSTARRS surveys (the field is not covered by Catalina). We found that the GROND object has been detected only once in ZTF but repeatedly in PannSTARRS. We carried out a periodicity search in this data using the same approach as described in Section 3.4. However, the number of observations obtained with PanSTARRS is still too small to allow the detection of a significant optical modulation. Therefore, we cannot add information on the light curve characteristics of the candidate optical counterpart proposed by Salvetti et al. (2017) and on their possible long-term evolution. Dedicated follow-up observations, aimed at a radial velocity measurement and an X-ray detection, are needed to verify its association with 4FGL J0744.0−2525 and confirm that this γ-ray source is indeed an RB candidate.

4.4 X-ray variable BW/RB candidates

Like we explained in Section 3.5, we carried out a systematic search for both periodic and aperiodic X-ray variability with the *EXTraS* tools[8] for all the 41 *XMM–Newton* sources detected in the fields of 13 γ-ray sources (Table 1). This we did regardless of an association with either known BW/RB candidates or other types of pulsars and of the association with an optical counterpart in the reference surveys, which makes our analysis bias-free. We note that the data products from the *EXTraS* variability analysis available online in the *EXTraS* archive[9] are still based on observations included in 3XMM catalogue releases earlier than DR8, mostly DR4 (up to December 2012) and DR5 (up to December 2013), which were the reference at the time the *EXTraS* project was carried out (2014–2016). Therefore, a major part of this work was to run the *EXTraS* variability analysis off-line to extend the results to all observations included in 3XMM/DR8 (up to November 2017).

---

[8] See http://www.extras-fp7.eu/index.php/archive to access the tool documentation.
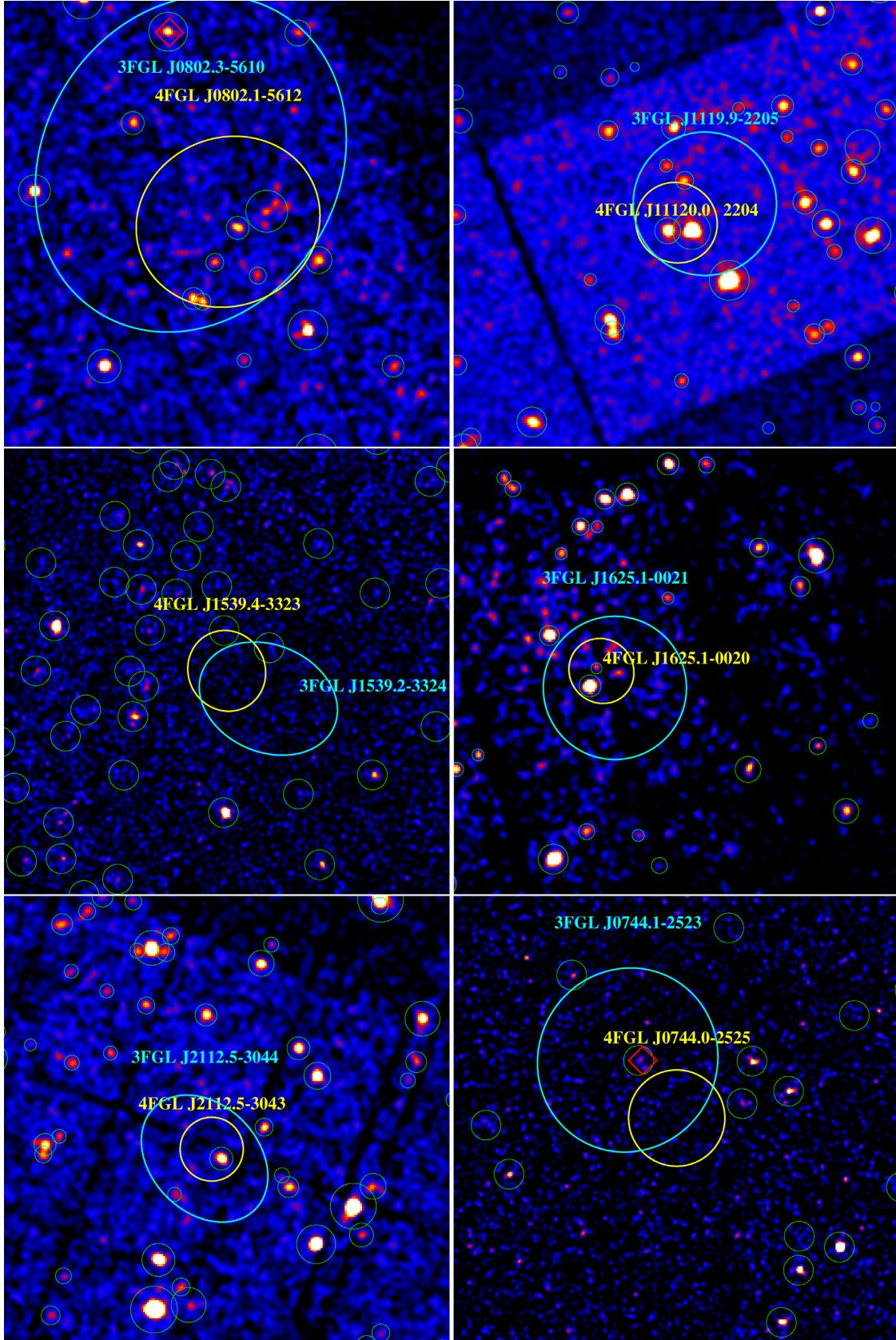[9] https://www88.lamp.le.ac.uk/extras/archive

Figure 12. 3FGL and the 4FGL error ellipses (cyan and yellow, respectively) for the γ-ray MSP candidates described in Section 4.3 overlaid on the X-ray image from either *XMM–Newton* or *Swift* (4FGL J0744.0−2525 and 4FGL J1539.4−3323) smoothed with a Gaussian filter (three pixel radius). All images are 0°.25 × 0°.25 in size. Sources from the XMM-DR8 and 1SXPS catalogues are marked by the green circles For both 4FGL J0802.1−5612 and 4FGL J0744−2525 the position of the candidate optical counterparts of Salvetti et al. (2017) is marked by the red diamond.

4.4.1 Transient and aperiodic X-ray variability

First of all, to make sure that we did not miss potential X-ray counterparts to the γ-ray MSP sources we used the off-line *EXTraS* tools to search for X-ray sources with flaring activity characterised by rapid transitions from 'off' to 'on' states within the same *XMM–Newton* observation. These are sources that switch from count rates below the detection threshold to count rates well above it, which might escape automatic source detection and do not end up in the 3XMM catalogue (see Section 3.5). After setting the detection threshold to 200 counts in the 0.3–10 keV energy band and the maximum flare duration to 10 ks, we indeed found one such flaring sources, which is not in the 3XMM/DR8 catalogue. In particular, we discovered this source in the *XMM–Newton* observation (OBS ID 0112200301; 29.6 ks) of the γ-ray source 4FGL J0359.4+5414, now identified as the isolated young γ-ray pulsar PSR J0359+5414 (Clark et al. 2017), with a flare duration of $\sim$3.8 ks. This source, however, is at coordinates $\alpha = 03^{\rm h}58^{\rm m}49\overset{\rm s}{.}73$; $\delta = +54^\circ 12' 54\overset{''}{.}7$ and, whatever its nature, it is clearly not associated with the pulsar which is at $\alpha = 03^{\rm h}59^{\rm m}26\overset{\rm s}{.}01$; $\delta = +54^\circ 14' 55\overset{''}{.}7$ (Clark et al. 2017). No other 'on/off' flaring source has been detected in the *XMM–Newton* observations of the fields of the remaining 12 γ-ray sources.

Incidentally, we note that source 3XMM J035925.2+541455 lies at only 7 arcsec (slightly larger than our assumed matching radius, Section 3.3) from the position of 2CXO J035926.0+541455 (Table 1), which is the candidate X-ray counterpart to PSR J0359+5414 detected by Zyuzin, Karpova & Shibanov (2018) in a $\sim$460 ks *Chandra* observation. The source is at the centre of a 30-arcsec-long extended X-ray emission which might have not been fully resolved by *XMM–Newton*, affecting its accuracy on the source position determination and the match with the *Chandra* one. Thus, it seems most likely that the X-ray counterpart to PSR J0359+5414 has also been detected by *XMM–Newton*. Due to the shorter exposure time, however, this observation would not add more information on the X-ray emission of PSR J0359+5414 with respect to the *Chandra* one.

Using an updated version of the *EXTraS* tools (Marelli et al. 2017), we also searched for both flares and other types of short-term aperiodic variability in X-ray sources which are always in an 'on' state within the same observation. Briefly, these tools employ a quantitative analysis of the X-ray light curve to spot deviations from a constant flux level as well as possible trends, such as flux modulations caused by either an intrinsic source periodicity or by the source eclipse. Only X-ray sources with at least 100 counts in the combination of the PN/MOS1/MOS2 detectors and classified as point-like according to their 3XMM/DR8 extension parameter are considered in the *EXTraS* analysis. We found a bright X-ray flare only for 3XMM J083850.4−282757, associated with the RB candidate 4FGL J0838.7−2827, with a flare duration of $\sim$600 s (see Fig. 13). This is the same flaring source pinpointed by Halpern et al. (2017a), which proves that the automatic *EXTraS* procedure that we applied in the search for flares works effectively.

4.4.2 Periodic X-ray variability

We used the *EXTras* tools also to search for *XMM–Newton* sources with evidence of periodic variability, starting from the counterparts to the known BW/RB candidates (Table 1). Only four of them have been detected by *XMM–Newton*. In the same 4FGL J0838.7−2827 field, we recovered the orbital and superorbital flux modulations observed in the X-ray source 3XMM J083843.3−282701 (OBS ID 0764420101 and 0790180101), identified with the Cataclysmic
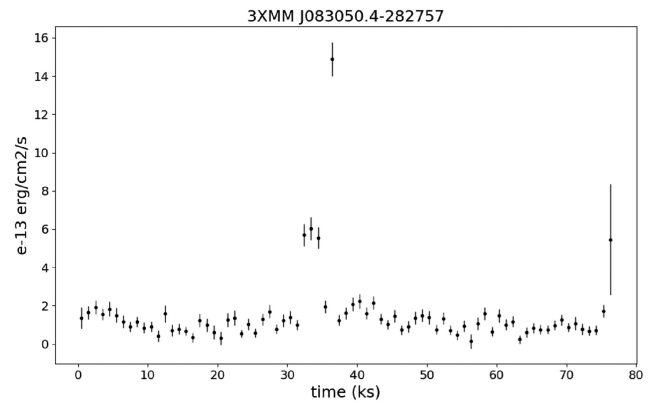

Figure 13. X-ray light curve of 3XMM J083850.4−282757, with a binning of size 997 s, in which appears a bright flare of duration of about 600 s, see also Halpern et al. (2017a).
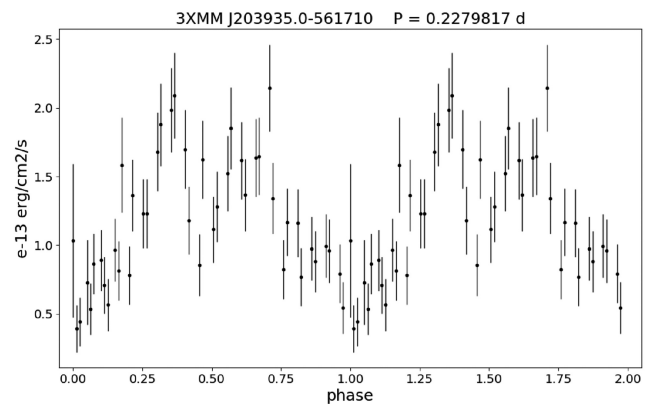

Figure 14. X-ray light curve of 3XMM J203935.0−561710, the X-ray counterpart to the γ-ray source 4FGL J2039.5−5617 folded at the orbital period computed by Strader et al. (2019).

Variable Star 1RXS J083842.1−282723 (Halpern et al. 2017a). However, we did not find evidence of periodic flux modulations in 3XMM J083850.4−282757, the one associated with the γ-ray source, before and after subtracting the contribution of the bright X-ray flare. As for the known BW/RB candidates with a measured optical periodicity (Table 2), we recovered the periodic X-ray flux modulation ($\sim$0.22d) in 3XMM J203935.0−561710 (OBS ID 0720750301), the X-ray counterpart to the RB candidate 4FGL J2039.5−5617 (Salvetti et al. 2017). The modulation (see Fig. 14) is more clearly recognised after folding the X-ray data at the orbital period of the binary system measured by Strader et al. (2019). We also found a trend of a more or less regular X-ray flux modulation in the unfolded light curve of 3XMM J154439.4−112804 (OBS ID 0724080101; 42.2 ks), as shown in Fig. 15 (top), the X-ray counterpart to the candidate tMSP 4FGL J1544.5−1126 (Bogdanov & Halpern 2015). The X-ray light curve folded at the orbital period of the binary system, $P_{\rm orb} = 0.2415361$ d (Britt et al. 2017) is also shown in Fig. 15 (bottom). Most likely, however this modulation is due to the X-ray flux bi-modality observed during the observation (Bogdanov & Halpern 2015), when the source was in a low-luminosity accretion state. Observations obtained in a non-accreting state would give a better chance to discover a genuine orbital periodicity in the X-ray flux of 3XMM J154439.4−112804. Finally, for the binary MSP and possible BW candidate 4FGL J1946.5−5402 (PSR J1946−5403) we
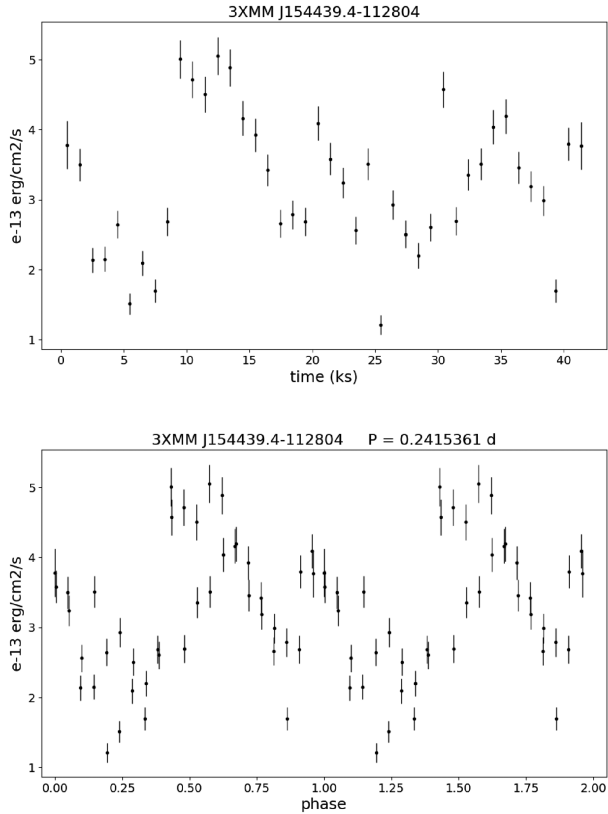
Figure 15. (Top) Unfolded X-ray light curve of the X-ray source 3XMM J154439.4−112804, with a binning of size 997 s. (Bottom) X-ray light curve folded at the orbital period of the binary system (Britt et al. 2017).

reported a tentative optical flux modulation in its possible counterpart SSS J194633.7−540236 but only after folding the Catalina data at the orbital period of the binary system (0.13 d; Section 4.1). We failed to find clear evidence of flux periodicity in the associated X-ray source 3XMM J194633.6−540236 (OBS ID 0784771001; ∼20 ks), with only a possible hint of an ∼0.13 d modulation recognised in the unfolded light curve. An *XMM–Newton* observation longer than the one currently available is needed to fully cover at least two orbital cycles and investigate this possible periodicity.

We searched for evidence of X-ray periodicity among the six candidate γ-ray MSPs with a possible *XMM–Newton* counterpart For 3XMM J210350.0−111338 (OBSID 0041150101 and 0041150201) we only see a very marginal evidence of variability in the X-ray light curve. For the remaining five candidate γ-ray MSPs with a possible *XMM–Newton* counterpart, with or without an associated optical counterpart (4FGL J0802.1−5612, 4FGL J1120.0−2204, 4FGL J1625.1−0020, 4FGL J2112.5−3043, and 4FGL J2333.1−5527), we found no evidence of periodicity in our blind search. The first four of these X-ray sources were preliminary searched for variability/periodicity by Salvetti et al. (2017) who found no evidence in either directions. Our analysis based on the *EXTraS* tools confirms their results.

Of course, we did not find any evidence of orbital periodicity in the *XMM–Newton* data of the three known isolated γ-ray pulsars (Table 1), i.e. the young pulsar PSR J0359+5414 (4FGL J0359.4+5414) and the two MSPs PSR J1035−6720 (4FGL J1035.4−6720) and PSR J1744−76194 (4FGL J1744.0−7618), which we used as a yardstick to sort out doubtful cases.

4.4.3 Long-term X-ray variability

Finally, we searched for possible long-term X-ray variability for all the 41 *XMM–Newton* sources in our sample. Since it was not possible for us to re-run off-line the dedicated *EXTraS* long-term X-ray variability analysis, we browsed the dedicated on-line *EXTras* data products archive, which is still based on observations included in the 3XMM/DR5. For this reason, for some sources we could not find corresponding data products. For the others we found that none deviates from a steady flux in any of the analysed energy bands. The lack of evidence of long-term X-ray variability can be explained in some cases by the steady source nature, in others by an insufficiently long multi-epoch coverage.

5 SUMMARY AND CONCLUSIONS

Using archival data and source catalogues, we carried out a multi-wavelength survey of the 48 MSP candidates selected from unassociated 3FGL sources by Saz Parkinson et al. (2016), based on machine-learning techniques. We found that 23 of these MSP-like γ-ray sources have candidate X-ray counterparts in *XMM–Newton*, *Chandra*, or *Swift*,[10] of which 17 are associated with an optical counterpart in at least one of the multi-epoch surveys. Six of them show evidence of optical periodicity with a period smaller than 1 d, detected through a blind search. We could recover the known optical periodicity for four confirmed BWs/RBs (4FGL J0523.3−2527, 4FGL J0955.3−3949, 4FGL J1653.6−0158, 4FGL J2039.5−5617), which proves the validity of our analysis. For two MSP candidates (4FGL J1627.7+3219 and 4FGL J2212.4+0708), we found a candidate optical periodicity for the first time, which needs to be confirmed by follow-up observations, making them BW/RB candidates. We also revisited the optical identifications for two binary MSP candidates of Saz Parkinson et al. (2016), now 4FGL J0802.1−5612 and 4FGL J0744.0−2525, proposed in Salvetti et al. (2017) on the basis of a periodic flux modulation. For the former, the proposed candidate counterpart now falls far from the updated γ-ray error ellipse and cannot be associated with 4FGL J0802.1−5612 any longer. For the latter, the candidate counterpart only falls marginally outside (∼15 arcsec) the 4FGL error circle and the association cannot be firmly ruled out. The periodicity could not be detected in the sparse multi-epoch optical survey data, so that we cannot investigate any long-term evolution of the orbit. An X-ray detection would be crucial to determine the nature of the proposed optical counterpart and verify its association with 4FGL J0744.0−2525.

We made use of the *EXTraS* tools to run an X-ray variability analysis of our γ-ray MSP candidates in the *XMM–Newton* data, including the search for orbital periodicity and flares. Although we could recover known phenomena, e.g. the X-ray orbital modulation in the RB candidate 4FGL J2039.5−5617 and the X-ray flare in the RB candidate 4FGL J0838.7−2827, these remain the only clear cases. Not surprisingly, the detection of X-ray modulations with a few hour period requires comparably long observations, whereas the detection of X-ray flares would benefit of a regular monitoring.

Our BW/RB identification score (four confirmed plus two candidates out of the 23 examined MSP-like γ-ray sources) would be higher than expected from the fraction of binary MSPs that are firmly identified as BWs/RBs (≈20 per cent) even if one assumes

---

[10]When our manuscript was about to be submitted an updated version of the *Swift* X-ray source catalogue (2SXPS; Evans et al. 2020) was published. We will update our work in the future using this catalogue as well as new releases of the *XMM–Newton* and *Chandra* X-ray source catalogues.

that the γ-ray sources in our sample are all MSPs, with at least one known exception (i.e. 4FGL J0359.4+5414 identified with the isolated young pulsars PSR J0359+5414; Clark et al. 2017), and that the corresponding fraction of binary ones is the same as in the entire MSP population ($\approx$65 per cent). Our identification score would be even more unexpected if one considers that our identification efficiency is affected by observational biases, such as the multiwavelength coverage extent (both spatially and temporally) of the γ-ray error ellipses of the MSP candidates (Section 3.2). Interestingly, in γ-rays the number of identified BWs/RBs relative to the total number of binary MSPs is $\approx$ 40 per cent, i.e. above the overall $\approx$20 per cent fraction, implying that a sample selection based on the γ-ray detection may introduce a statistical bias. As previously said, however, the identification of our two new BW/RB candidates still awaits confirmation, which might downplay the statistical impact of our results.

We plan to update our work once new MSP candidates are selected by machine-learning techniques (e.g. Saz Parkinson et al. 2016) from new *Fermi* source catalogue releases, starting from the 4FGL, exploiting the growing multiwavelength survey databases and a more systematic mining of archival data. One of the reference for future works would be the list of γ-ray MSP candidates from the 4FGL published by Luo et al. (2020) when this works had been just finalised. On a longer run, future systematic searches will greatly benefit from the data stream of X-ray/optical survey facilities, such as *e-Rosita* on the *Spectrum Röntgen Gamma* satellite, launched in July 2019, and the Large Synoptic Survey Telescope, now Vera C. Rubin Observatory, with routine observations scheduled start in 2022.

DATA AVAILABILITY

The data used in this work are all available in public archives.

REFERENCES

Abdollahi S. et al., 2020, ApJS, 247, 33
Acero F. et al., 2015, ApJS, 218, 23
Alpar M. A., Cheng A. F., Ruderman M. A., Shaham J., 1982, Nature, 300, 728
Archibald A. M. et al., 2009, Science, 324, 1411
Atwood W. B. et al., 2009, ApJ, 697, 1071
Backer D. C., Kulkarni S. R., Heiles C., Davis M. M., Goss W. M., 1982, Nature, 300, 615
Bellm E. C. et al., 2018, PASP, 131, 018002
Bogdanov S., Halpern J. P., 2015, ApJ, 803, L27
Bonanos A. Z. et al., 2019, A&A, 630, A92
Britt C. T., Strader J., Chomiuk L., Tremou E., Peacock M., Halpern J., Salinas R., 2017, ApJ, 849, 21
Bruel P., Burnett T. H., Digel S. W., Johannesson G., Omodei N., Wood M., 2018, preprint (arXiv:1810.11394)
Camilo F. et al., 2015, ApJ, 810, 85
Chambers K. C., Pan-STARRS Team, 2016, in American Astronomical Society Meeting Abstracts #227, p. 324.07
Cho P. B., Halpern J. P., Bogdanov S., 2018, ApJ, 866, 71
Clark C. J. et al., 2017, ApJ, 834, 106
Clark C. J. et al., 2018, Sci. Adv., 4, eaao7228
Dai X.-J., Wang Z.-X., Vadakkumthani J., Xing Y., 2016, Res. Astron. Astrophys., 16, 012
Dai X.-J., Wang Z.-X., Vadakkumthani J., Xing Y., 2017, Res. Astron. Astrophys., 17, 072
De Luca A., Salvaterra R., Tiengo A., D'Agostino D., Watson M. G., Haberl F., Wilms J., 2016, in Astrophysics and Space Science Proceedings, Springer International Publishing, Switzerland, p. 291
Evans I. N. et al., 2010, ApJS, 189, 37
Evans P. A. et al., 2013, ApJS, 210, 8
Evans P. A. et al., 2020, ApJS, 247, 54
Fruchter A. S., Stinebring D. R., Taylor J. H., 1988, Nature, 333, 237
Halpern J. P., Bogdanov S., Thorstensen J. R., 2017a, ApJ, 838, 124
Halpern J. P., Strader J., Li M., 2017b, ApJ, 844, 150
Hui C. Y., Li K. L., 2019, Galaxies, 7, 93
Jaodand A., Hessels J. W. T., Archibald A., 2016, in Weltevrede P., Perera B. B. P., Preston L. L., Sanidas S., eds, The Universe of Digital Sky Surveys, Astrophysics and Space Science Proceedings, Vol. 42. Springer International Publishing, Switzerland, p. 291
Kulkarni S. R., 2013, Astron. Telegram, 4807, 1
Lansbury G. B. et al., 2017, ApJ, 846, 20
Larson S., Beshore E., Hill R., Christensen E., McLean D., Kolar S., McNaught R., Garradd G., 2003, in AAS/Division for Planetary Sciences Meeting Abstracts #35, p. 3
Li K.-L. et al., 2018, ApJ, 863, 194
Linares M., 2014, ApJ, 795, 72
Linares M., 2019, preprint (arXiv:1910.09572)
Luo S., Leung A. P., Hui C. Y., Li K. L., 2020, MNRAS, 492, 5377
Marelli M. et al., 2017, ApJ, 851, L27
Mignani R. P., 2011, Adv. Space Res., 47, 1281
Mignani R. P. et al., 2014, MNRAS, 443, 2223
Ng C. W., Takata J., Strader J., Li K. L., Cheng K. S., 2018, ApJ, 867, 90
Pletsch H. J. et al., 2012, Science, 338, 1314
Radhakrishnan V., Srinivasan G., 1982, Curr. Sci., 51, 1096
Rau A. et al., 2009, PASP, 121, 1334
Ray P. S. et al., 2013, ApJ, 763, L13

Ray P. S. et al., 2016, American Astronomical Society Meeting Abstracts #227, p. 423.07

Ray P. S. et al., 2020, Res. Notes Am. Astron. Soc., 4, 37

Rea N. et al., 2017, MNRAS, 471, 2902

Roberts M. S. E., 2011, An Astrophysical Key to Unlock the Secrets Of the Universe, Vol. 1357, AIP Conference Proceedings, p. 127

Romani R. W., 2015, ApJ, 812, L24

Romani R. W., Filippenko A. V., Cenko S. B., 2014, ApJ, 793, L20

Rosen S. R. et al., 2016, A&A, 590, A1

Salvetti D. et al., 2015, ApJ, 814, 88

Salvetti D. et al., 2017, MNRAS, 470, 466

Saz Parkinson P. M., Xu H., Yu P. L. H., Salvetti D., Marelli M., Falcone A. D., 2016, ApJ, 820, 8

Strader J., Chomiuk L., Sonbas E., Sokolovsky K., Sand D. J., Moskvitin A. S., Cheung C. C., 2014, ApJ, 788, L27

Strader J. et al., 2019, ApJ, 872, 42

Süveges M., 2014, MNRAS, 440, 2099

Torres D. F., Ji L., Li J., Papitto A., Rea N., de Oña Wilhelmi E., Zhang S., 2017, ApJ, 836, 68

VanderPlas J. T., Connolly A. J., Ivezic Z., Gray A., 2012, Proceedings of Conference on Intelligent Data Understanding, IEEE, p. 47

VanderPlas J. T., Ivezić, Ž., 2015, ApJ, 812, 18

Wang P. et al., 2018, Astron. Telegram, 11584, 1

Yao J. M., Manchester R. N., Wang N., 2017, ApJ, 835, 29

Zyuzin D. A., Karpova A. V., Shibanov Y. A., 2018, MNRAS, 476, 2177

This paper has been typeset from a TEX/LATEX file prepared by the author.